# Drying droplet as a template for solid formation

Roger Williams de Souza Lima, Maria-Inês Ré, Patricia Arlabosse

# Drying droplet as a template for solid formation: A review

R. de Souza Lima*, M.-I. Ré, P. Arlabosse

*Université de Toulouse, IMT Mines Albi-Carmaux, CNRS UMR 5302, Centre RAPSODEE, Campus Jarlard, 81013, Albi, CEDEX 09, France*

*Keywords:*
Droplet template
Drying droplet
Multi-component solid systems
Spray-drying
Particle morphology
Experimental and modeling approaches

A B S T R A C T

Multi-component liquid droplets are useful systems to design particles with engineered solid structures by spray drying. However, the use of such process still presents some scientific challenges, such as the development of a model to precisely describe the final particle structure from the initial drying conditions and liquid formulation.

This review brings together experimental and modeling studies that have been developed in the literature over the few last decades for a better understanding of the process of particle formation from a drying liquid droplet. To overcome such challenges, experimental studies at the spray scale and at the droplet scale have been proposed. Furthermore, modeling approaches have been suggested to represent the process of particle formation. The main existing models are well established for the first droplet drying phase, however, the processes of crust formation and development are more complex, which leaves space for further improvement of the proposed models.

**Contents**

1. Introduction ..... 161
2. A qualitative view on typical spray-dried particle solid structures ..... 162
3. Experimental approaches on drying droplets ..... 163
   3.1. At the spray scale ..... 163
   3.2. At the droplet scale ..... 164
      3.2.1. Presentation of the drying techniques ..... 164
      3.2.2. Suspension by a filament ..... 164
      3.2.3. On a hydrophobic surface ..... 166
      3.2.4. Acoustic levitation ..... 166
      3.2.5. Aerodynamic levitation ..... 166
      3.2.6. The free-fall technique ..... 166
      3.2.7. *In situ* component distribution evaluation ..... 166
4. Modeling approach for a single droplet ..... 167
   4.1. Empirical approach ..... 168
   4.2. Deterministic approach ..... 168
5. Perspectives and conclusion ..... 169
   References ..... 169

## 1. Introduction

Liquid droplets, which are afterwards solidified by physical or chemical transformations, is one of the major means of generation of solid particles with controlled properties like shape (predominantly spherical), size, chemical surface composition, porosity or density [1,2]. These properties impact other targeted functional solid properties, such as reactivity, dissolution and release profiles, taste masking, flowability or wettability [2,3], which are the main issues for applications including pharmaceutical [4], food [5], catalysis [6], development of new materials [7] and other fields [8–10].

* Corresponding author. IMT Mines Albi-Carmaux, CNRS UMR 5302, Centre RAPSODEE, Campus Jarlard, 81013, Albi, CEDEX 09, France.
*E-mail address:* rogerlima.w@gmail.com (R. de Souza Lima).

Liquid droplets as templates for solid formation are encountered with a variety of industrial processes, among them, spray drying. Spray drying involves the breaking of a liquid by a controlled liquid-gas dispersion achieved mechanically, pneumatically or ultrasonically [1,11–13] to produce droplets of well-controlled shape and size, which will become solid particles into the drying chamber. From spray drying, liquid droplets can be structured in sophisticated solid particles (e.g. porous, multi-layered coated, surface comprising smaller sub-units such as nanoparticles), which has attracted attention to the use of this technology in different fields of application [2,4,7,14].

Spray drying has been an interesting process for industrial applications over the years. This increasing attention can also be seen by the number of different papers published on this drying topic. In the Web of Science, more than one thousand papers are published every year. However, there are still a deficiency concerning the description of the particle formation in the spray drying operation, especially with multi-component systems containing compounds which have different physicochemical properties like water solubility, molecular mass, surface active properties or chemical polarity. Due to the interactions between the components caused by these differences, component separation might take place in a droplet during spray drying. The redistribution can be driven by the difference in the diffusivity of the components, component solubility, density, surface activity and hydrophobicity of components and the final composition within the dried particle is a resultant of all these forces.

The major scientific obstacle nowadays for designing multi-component solid particles is the detailed description of the component's distribution inside the droplet/wet particle during drying, besides prediction of the final particle morphology. Experimental and modeling approaches are used in the literature in order to overcome this handicap. Both approaches are developed either on the spray scale, which means working with a pilot- or lab-scale spray dryer, or on the single droplet scale.

The main objective of the paper is to highlight the interest on experimental and modeling approaches to study the mechanisms leading to the formation of different solid structures from drying liquid droplets. Thus, the review starts by introducing the diversity of spray-dried solid particle structures that can be obtained when the liquid formulation and the operating conditions are changed in a spray drying process. Secondly, it presents the experimental studies on the spray of droplets and the drying of a single droplet, including *in situ* measurements for composition evaluation. Finally, it focuses on the modeling of a drying droplet, regarding the systems dried, the crust formation and particle morphologies simulated.

## 2. A qualitative view on typical spray-dried particle solid structures

In the spray drying process, evaporation firstly takes place at the surface of the droplet. In that way, the solvent molecules inside the liquid phase will move from the core of the droplet to its surface. The other substances present in the droplet are equally carried by this outward motion. Thus, the solvent removal leads to a solute enrichment at the surface of the droplet, until a solid phase (crust) begins to form. As the solvent removal progresses, the crust thickens and grows towards the center of the liquid phase.

One important parameter that arises when dealing with the process of particle formation is the capillary pressure, which is derived from the difference in the pressure inside and out the droplet and is related to the surface tension (a force that acts upon reducing the surface area of the droplet). At the beginning of drying, the droplet shrinks and the internal pressure increases as a result from solvent removal. However, once the crust is formed, the reduction in the droplet volume is hindered. Consequently, a growing pressure will be applied over the new-formed crust for balancing the internal droplet pressure. The crust at the droplet surface may be rigid or flexible, depending on the solutes molecular size, viscoelastic properties and molecular interactions [15,16]. Thus, depending on the mechanical properties of the crust, the increase in capillary pressure will play a fundamental role on the definition of the final aspect of the resulting solid particle.

Typical visual aspects or particle morphologies of spray-dried solid structures are shown in Fig. 1. The particles may present a dense [4,17] or a hollow core [18–20], a wrinkled surface [4,21,22] or they may acquire the shape of a doughnut [23,24] or a raspberry [14,23]. The generated structure may also be highly porous [4,23] or have a “hairy” surface [23]. The reasons for these differences are discussed hereafter.

Starting from dense (Fig. 1-a) and hollow (Fig. 1-b) particles: when the evaporation flux from a liquid droplet is faster than the solute enrichment at the droplet surface, the formation of a solid crust in the droplet surface is delayed and the resulting solid particle may present a dense core. On the other hand, if the solvent is removed from the droplet faster than the compounds diffusion towards the center of the droplet, a hollow core is most likely to appear [25]. As a result, the particles obtained via spray drying may have a dense (Fig. 1-a) or a hollow core (Fig. 1-b), even though the hollow particle is more easily obtained due to the fast solvent removal rates employed in this process.

A smooth spherical hollow particle is formed when the mechanical strength of the crust formed during drying can sustain the inward capillary pressure, driven by the moisture evaporation [26]. If the resultant capillary pressure does not deform the crust, this could lead to a reduction in the wet particle's internal pressure, which could promote the formation of a bubble [27]. Upon further removal of solvent, this centrally located bubble would increase in diameter until the inner particle surface is solidified. If the pressure difference across the crust deforms it, a wrinkled (Fig. 1-c) or doughnut-like (Fig. 1-d) morphologies will probably be obtained after drying [16]. In addition, crust inhomogeneities can induce the buckling phenomenon as well, as shown by Bahadur et al. [24]. The phenomenon of the particle surface deformation has been mainly studied on the drying of colloidal suspension systems [26–29].

Raspberry-like particles (Fig. 1-e) are the result of the drying of a liquid suspension. The nano- or microparticles in the liquid phase also follow the drying mechanisms as described previously, such as the surface enrichment, but lead to the formation of a rough surface due to the their bigger size, which can go as high as 650 nm [14]. Correspondingly, the hairy-particle (Fig. 1-f) are generally produced from suspensions under some specific conditions as described by Nandiyanto and Okuyama [23], where a carbon nanotube catalyst (CoPd nanoparticles) and boron nitride nanoparticles were immersed into an ethanol droplet. Without the catalyst, the boron nitride and ethanol mixture would form raspberry-like particles. The addition of the CoPd causes the decomposition of ethanol and formation of carbon nanotubes on the particle's surface.

As described by Vehring [4], highly porous particles (Fig. 1-g) are the result of the drying of an emulsion, where the dispersed phase (acting as the porous template) evaporates slower than the continuous phase. A stabilizing agent is generally necessary to avoid coalescence of the dispersed phase during drying in order to generate the structure shown in Fig. 1-g.

The first scientific effort to study spray-dried particle morphologies was done by Charlesworth and Marshall [30]. These authors performed a series of single-solute solution droplet drying experiments in order to give a set of different particle morphologies. This experimental approach was later applied by Walton and Mumford [31], with the drying of single-solute solutions, suspensions and multi-component emulsions. Furthermore, the same authors highlighted the production of particles with a hollow or a dense core, a smooth or wrinkled surface, depending on the initial

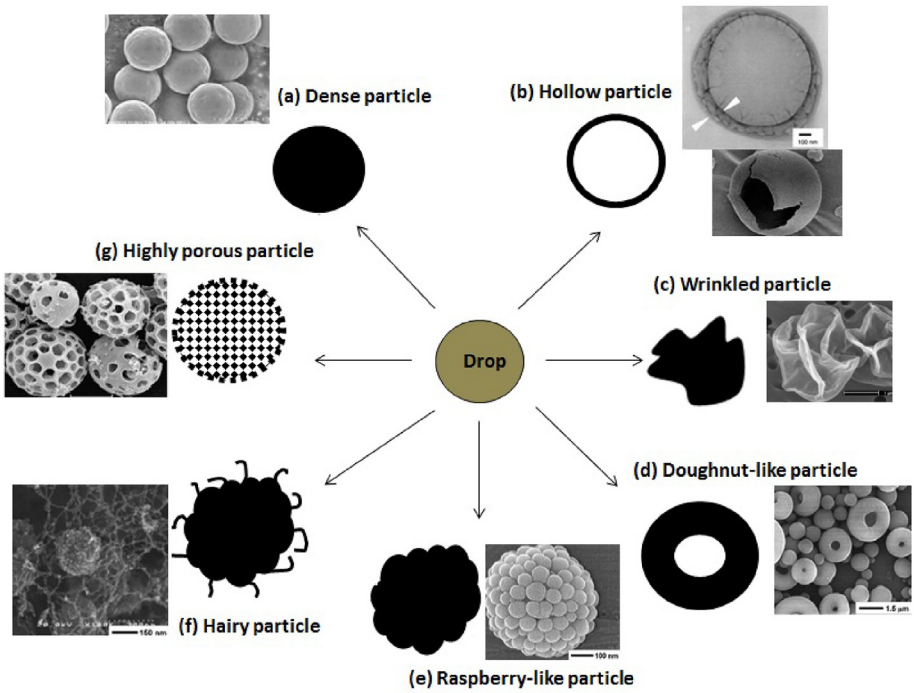


**Fig. 1.** A schematic representation of the possible particle morphologies obtained from the drying of a droplet: (a) dense core, (b) hollow core, (c) wrinkled particle, (d) doughnut-like particle, (e) raspberry-like particle, (f) hairy particle, (g) highly porous particle. Adapted with permission from Ref. [4]-(a,c,g) [18],-(b) [23],-(d,e,f).

liquid formulation and drying conditions. The reader may also consult a comprehensive review written by Nandiyanto and Okuyama [23] on the subject, with the production of different particle morphologies by varying the initial liquid formulation.

Regarding the application of the different morphologies presented in Fig. 1, Shah et al. [32] stated the use of particles with wrinkled surface for enhancing the aerosol performance in inhalation drug delivery systems due to a reduction in the attractive interparticle interactions. Such improvement in the pulmonary delivery efficiency could also be obtained from the low-density hollow particles [4]. For the highly-porous particle (Fig. 1-g), according to Vehring [4], the design of such particle with very low porosity have been applied for pulmonary delivery of small molecules and have been suggested for vaccination purposes.

The particle structures obtained via spray drying are strongly connected to the physicochemical properties of the substances being dried and the drying conditions. This Section highlighted the rich possibilities of particle morphologies that can be produced. In order to master the design of such tuned spray dried particles, regarding the morphology, the component distribution or mechanical resistance, for example, it is crucial to comprehend the mechanisms of particle formation, thus the importance of the experimental and modeling approaches presented in the next Sections.

## 3. Experimental approaches on drying droplets

In order to deal with the still present scientific challenges in the spray drying operation, two experimental approaches have been developed to study the drying of liquid droplets: either the experiments are focused on the spray of droplets, as in the industrial drying operation, or they are executed on a simplified version of the process, which means working with a single droplet.

### *3.1. At the spray scale*

Experimentally, understanding the drying mechanisms for a spray of droplets is based on the ability to relate the droplet properties before drying (e.g. droplet size, concentration) and the air properties (e.g. air inlet temperature, air flow), to the dried particle properties (e.g. particle apparent density, surface composition, porosity, morphology and inner component distribution), as shown in Table 1. The present approach is commonly accomplished with pilot- or lab-scale spray dryers [33]. Thus, the initial drying conditions are changed and the resulting effect on the final particle solid structure is analyzed by means of techniques like scanning electron microscopy, Raman spectroscopy, pycnometry and X-ray photoelectron spectroscopy. The main drawback of such approach is the lack of *in situ* monitoring to track changes in the composition of the droplets through the whole drying operation. This would require a technique sophisticated enough to follow the thousands of droplets of various sizes produced by the atomizer, transported by the air flow and dried in only a few seconds.

In order to follow the drying of the droplets, Pearce [34] presented a sampling device containing liquid nitrogen to flash frozen the droplets at different positions in the drying chamber. For each trial, the sampling device collected around 50−100 g of droplet/wet particles in a couple of minutes. The moisture content of the frozen sample was measured afterwards. Furthermore, air bulk properties, e.g temperature and humidity, can be measured from thermocouples and humidity sensors placed at different positions in the drying chamber, to obtain a discrete evolution of both air characteristics [35]. However, the droplet bulk properties measured with the device described by Pearce [34], along with the discrete evolution of the air characteristics, would give only a general idea about the drying history. In order to engineer solid particles from complex liquid formulations, a finer experimental evaluation of the solid formation mechanisms is required.

Hence, the drying of a single liquid droplet has been proposed as an alternative path to study the spray drying process. In that way, the structural evolution can be monitored and changes in the droplet properties can be quantified due to the use of bigger droplets, longer drying times and laboratory apparatus allowing the *in situ* follow-up [36,37]. A literature overview regarding the single droplet is the subject of the next section.

**Table 1**
A few examples of studies related to the effect of drying conditions and liquid formulations on particle properties at the spray scale.

| Authors | Compounds | Objective | Outcome |
|---|---|---|---|
| Poozesh et al. [124] | Solution of felodipine and polyvinylpyrrolidone in methanol | Qualitative analysis of the influence of the spray-dried particle size (produced from different solid loads, i.e. 0.63 %w/w and 2.4 %w/w) on particle morphology and porosity. | Larger particles (diameter greater than 20 μm) presented a porous structure with an important spatial dispersion of components. Smaller particles (diameter inferior to 10 μm) were more evenly distributed in composition and less porous. |
| Munoz-Ibanez et al. [3] | O/w emulsion. Sunflower oil as dispersed phase and acacia gum and maltodextrin as wall material. | Influence of the emulsion size (0.1 and 1 μm) and rotary atomizer speed (33200 rpm and 3270 rpm) on the particle morphology and component distribution. | The morphology changed from hollow and wrinkled to hollow and smooth by decreasing the atomizer speed. Oil droplets, in general, evenly distributed in the particle crust. Increasing the atomizer speed had a positive effect on the wall material spatial distribution. |
| LeClair et al. [125] | Aqueous solution of mannitol, dextran and adenovirus expressing Escherichia coli $\beta$-galactosidase. | Influence of spray drying parameters (air inlet temperature, gas flow rate, liquid feed flow rate and initial solute concentration) on powder yield, particle size fraction below 5 μm and viral vector activity loss. | Loss in viral activity was affected mainly by an increase in the air inlet temperature and gas flow rate. A reduction in powder yield and the desired particle size fraction was the result of increasing the air inlet temperature, the liquid feed flow rate and the initial solute concentration. An increase in the gas flow rate had no significant effect on the powder yield, but increases the desired particle size fraction (5 μm). |
| Bahadur et al. [24] | Colloidal dispersion of silica and a polymer (polyethylene glycol) with two different molecular weights (PEG400 or PEG1450). | Investigation of the particle morphology by changing the polymer and its concentration (0.5, 1.0, 2.0 and 3.0% w/w). | Pure silica particle had a doughnut shape. Adding 0.5% w/w of PEG400 led to a spherical particle with a small dimple. Higher concentrations resulted in spherical particles. Using PEG1450 at 0.5% w/w resulted in spherical particles. Higher concentrations generated wrinkled particles. |
| Li et al. [21] | O/w emulsion. Vitamin E as oil phase. Wall materials: whey protein, maltodextrin, gum arabic, Nutriose, Kleptose or Cleargum. | Analysis of pure wall material morphology and size distribution. Effect of adding vitamin E to the morphology and size distribution of whey protein, as model wall material. Investigation of the size of the vitamin E nanodroplets before and after spray-drying. | The pure wall materials produced wrinkled particles with size ranging from 1.5 μm to 2.0 μm. The wrinkled particle of pure whey protein became a smooth spherical particle by the addition of vitamin E. Changing the vitamin E concentration from 21.4% to 17.6% w/w reduced the particle size from 2.0 μm to 500 nm. The vitamin E nanodroplets doubled in size after spray-drying compared to the initial emulsion size. |
| Elversson and Millqvist-Fureby [19] | Aqueous solutions of lactose, mannitol and sucrose/dextran. | Investigation of the influence of feed concentration (ranging from 1% w/w to the corresponding saturation concentration) on particle size and apparent density. The effect of changing the dissolved solids on particle morphology was also examined. | Higher solid contents resulted in bigger particles and lower apparent density. Lactose and sucrose/dextran originated hollow amorphous particles. Mannitol alone produced crystalline porous particles. |
| Steckel and Brandes [20] | Oil-in-water emulsion. Aqueous phase composed of salbutamol sulphate, poloxamer (or phosphatidylcholine) and lactose (or a cyclodextrin derivative). Oil phase composed of HPCD (2-hydroxypropyl-beta-cyclodextrine) or HPCD + dichloromethane. | Creation of particles with low apparent density for pulmonary drug delivery by changing the volatility of the emulsion oil phase. | Particles with an apparent density of 0.04gcm$^{-3}$ were obtained with only HPCD in the oil phase. Particles were hollow with a thin shell and a blow-out hole. Adding dichloromethane to the oil phase reduced the particle apparent density to 0.02gcm$^{-3}$. The new particles presented a highly porous structure. |
| Elversson et al. [18] | Aqueous solution of lactose | Effect of nozzle diameter (1.5 mm and 2.0 mm), atomization air flow (from 20.6Lmin$^{-1}$ to 35.7Lmin$^{-1}$) and feed solid content (from 1% w/w to 20% w/w) on droplet and particle size | Droplet size controlled by nozzle diameter and air flow. Particle size increased by higher nozzle diameter and feed concentration. |

### 3.2. At the droplet scale

#### 3.2.1. Presentation of the drying techniques

Changing the observation scale, from a spray of droplets to a single droplet, has become an interesting route to understand the mechanisms of component interaction and distribution inside the liquid droplet and the formation of the solid structure. As presented in Fig. 2, the single droplet will clearly not experience the same drying conditions as it would in the industrial drying chamber – especially with the increase in droplet diameter (achieving droplet sizes ten times bigger than that in the industrial chamber) [38] and drying time (from seconds in the industrial chamber to minutes in the single drop experiment) and the suppression of the disturbances related to the spray drying process (e.g. droplet-to-droplet interaction, droplet-to-wet particle interaction, droplet-chamber wall collision) [37]. Nevertheless, single droplet experiments can still be used to reproduce particle morphologies that would be obtained from the industrial process [16,39].

Many devices have been presented in the literature to follow the drying of a single droplet (Fig. 3). Some use an intrusive material to hold the droplet in place, like a filament [40–43] or a hydrophobic surface [44–47]. Others maintain the droplet's position by means of an acoustic field [48–51] or an air stream [52–54]. A droplet can also be let to freely fall through a small chamber [55–57]. Less common methods consist of placing the droplet between plates [58] or making it levitate on a thin layer of its own vapor (the Leindenfrost effect) [26].

The proposed devices tend in their ways to reproduce the environment encountered by the droplets in the industrial drying chamber, apart from the collisions. As a consequence, they are useful to give detailed technical information but also have inherent limitations, as summarized in Table 2. The choice of the method will depend on the researcher's judgment in weighting the suitability of the method to the goal of the study.

#### 3.2.2. Suspension by a filament

Regarding the method of droplet suspension by a filament, the droplet mass variation over time can be accurately measured by attaching the filament to a precision balance, provided that special attention is given to the air flow disturbances on the mass recording. The filament method has been used for droplets containing dissolved salts [43,59,60], dissolved sugars [41,61,62],

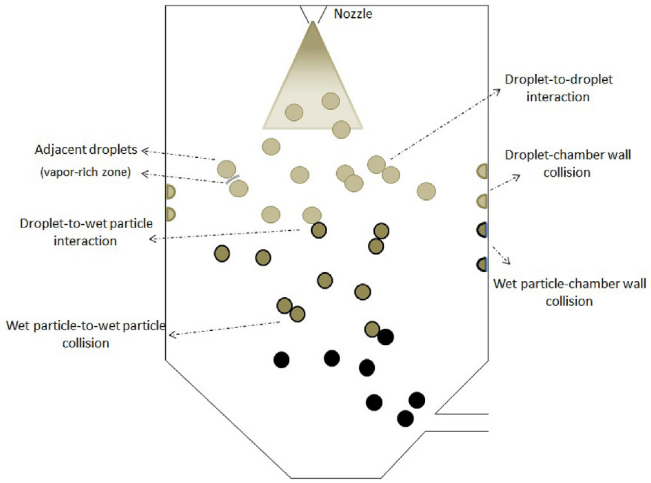


**Fig. 2.** Representation of the disturbances that occur during the drying of liquid droplets in the spray-drying chamber.

functional oils [63,64], pharmaceutical compounds [65,66] or droplets containing milk components [42,67–71]. A thermocouple may be inserted in the droplet in order to assess its temperature, as accomplished by Al-Mubarak et al. [72] and Lin and Chen [42]. This adds another intrusive material in the interior of the liquid phase, which can interfere in the drying of the droplet. To overcome the use of a thermocouple, Saha et al. [73] used an infrared camera with a droplet levitated by acoustic waves, but only the droplet surface temperature could be measured.

The intrusive material used to hold the droplet in place must cause the least possible disruption to the drying of the droplet. In that way, Han et al. [74] et Fu et al. [39] examined the effect of the suspension filament on the energy transferred by conduction to the droplet during drying. They showed that the presence of a glass filament only contributes to approximately 1% of the total heat transferred to a 1 mm droplet. However, this low energy input could still be considered as a parasite heat transfer [75]. Regarding the effect of the filament on the mass transfer, the presence of scratches on the surface may promote heterogeneous nucleation, which offers a smaller energy barrier for phase transition. In that way, the particle solid structure may be formed sooner than in the case without the filament. Thus, it may influence the final particle diameter and at a lesser extent the distribution of the components in the solid structure.

In an industrial drying chamber, the air flowing around a droplet presents homogeneous temperature and vapor content profiles due to the turbulent flow. In that way, heat and mass transfers are more symmetrical over the surface of the droplet. However, in the single droplet methods, the air flows in a laminar regime. Thus, the heat and mass transfers are greater on the droplet side facing the air

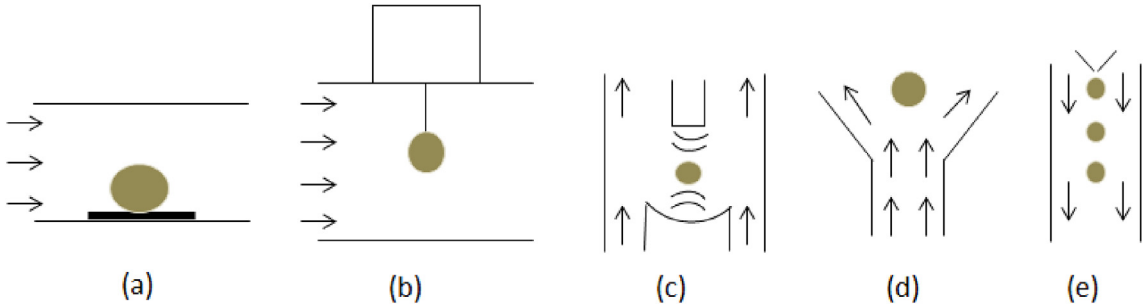


**Fig. 3.** Single droplet drying techniques: (a) droplet on a hydrophobic surface; (b) droplet hanging on by filament; (c) droplet levitated in a acoustic levitator; (d) droplet levitated by an air flow; (e) free-fall technique.

**Table 2**
Single droplet drying techniques: an overview.

| *Non-invasive methods* | | | *Invasive methods* | |
|---|---|---|---|---|
| Chain of droplets | Aerodynamic levitation | Acoustic levitation | Thin filament | Hydrophobic surface |
| *Available information* | | | | |
| Diameter evolution tracking | Diameter evolution tracking | Diameter evolution tracking | Diameter evolution tracking | Diameter evolution tracking |
| Radial composition measurement | Radial composition measurement | Radial composition measurement | Radial composition measurement | Radial composition measurement |
| – | Droplet temperature assessment | Droplet temperature assessment | Droplet temperature assessment | Droplet temperature assessment |
| – | – | – | Droplet mass determination | Droplet mass determination |
| – | – | – | – | Crust growth observation |
| – | – | – | – | Droplet's internal structure visualization |
| *Technical limitations* | | | | |
| No direct temperature measurement | – | – | – | – |
| No direct mass measurement | No direct mass measurement | No direct mass measurement | – | – |
| – | – | Droplet position control | Droplet position control | – |
| – | – | Droplet size (300 μm - 1 mm) | Droplet size (500 μm - 9 mm) | Droplet size (150 μm - 2 mm) |
| – | – | Droplet deformation | – | Droplet deformation |
| – | – | – | Lack of free rotation | Lack of free rotation |
| – | – | Parasite heat transfer | Parasite heat transfer | Parasite heat transfer |
| – | Solute nucleation zone | Solute nucleation zone | Solute nucleation zone | Solute nucleation zone |

flow and lower on the wake region. To adress this issue, Hassan and Mumford [15] et Al-Mubarak et al. [72] used a rotating capillary to homogenize the mass and energy transfers, but the impact of the revolving speed on the evaporation rate was not investigated.

#### 3.2.3. On a hydrophobic surface

The other intrusive drying method consists of placing a droplet on a flat surface covered with a hydrophobic substance, like polydimethylsiloxane (PDMS) [46,76], polypropylene [77] or Teflon [45], so that a high contact angle can be obtained between the droplet and the surface. To increase even further the contact angle, Al-Shehri et al. [78] used a spinning hydrophobic surface to obtain a perfectly spherical droplet. This single droplet method has been used for investigating the inactivation of a bioactive substance during drying [47], surface buckling [27–29,77], vacuole formation and mechanical properties of milk particles [58,76], organisation [79], movement [80–82], agglomeration [44] of nanoparticles during drying and also droplet bouncing on hydrophobic surfaces [83–85].

Sadek et al. [76] placed an optical microscope in fluorescent mode near the hydrophobic surface to observe the solid structure formation inside the droplet containing a fluorescent dye. The images captured by the microscope corresponded to a horizontal plan 60 μm away from the hydrophobic surface.

Like the filament method, the hydrophobic surface may transfer heat by conduction to the droplet. According to Perdana et al. [47], this energy input is smaller than 5% of the total heat transferred to the droplet. The hydrophobic surface may also present preferential sites for solid nucleation. to Perdana et al. [47] also highlighted the modification of the air streamlines around the droplet (due to the presence of the surface) and the importance of appropriately adjust heat and mass transfer coefficients.

#### 3.2.4. Acoustic levitation

To avoid using an intrusive material to hold the droplet in place, an acoustic field can be created by a transducer and a reflector. A droplet inserted in this field will not move due to an equilibrium between the droplet weight and the upward acoustic radiation force [75]. It means that the droplet can move upwards due to moisture loss if the pressure radiation force is kept constant [49]. This vertical displacement can be used to generate the droplet drying curve [48]. The use of such method may not be appropriate for the falling drying rate period, where the droplet mass loss becomes smaller and thus the change in droplet position is less discernible. To reduce the effect of acoustic streaming generated by the acoustic field around the droplet, some authors have adapted the acoustic levitator so that an air flow could be used [48,51,75,86]. In that way, the moisture vapor would not be retained at the droplet's boundary layer. The droplet position on the acoustic levitator could become unstable if the air flow rate were increased to suppress the effect of the acoustic streaming on the droplet drying rate. The acoustic levitation has been used for studying the structural behavior of proteins during drying [87], particle mechanical strength [88,89], droplet velocity field [80,90] and surface buckling [91].

#### 3.2.5. Aerodynamic levitation

The aerodynamic levitator, as presented by Adhikari et al. [52], is another non invasive method used for the drying of single droplets. In this case, an air flow is created to suspend and dry the droplet. This method is rarely applied for drying droplet studies, due to the difficulties in maintaining the droplet in place, which makes the image capture and mass and temperature measurements difficult. However, in the field of physics, Weber et al. [54] and Hennet et al. [53] have used the aerodynamic levitation to study molten materials using synchrotron x-ray.

#### 3.2.6. The free-fall technique

The single droplet drying method that resembles the most the spray drying operation is the free-fall technique – or chain of droplets technique, when more than one droplet is produced during the experiment [57]. This method does not enable the direct measure of mass or temperature of the falling droplet. Image analysis has to be used to assess the evaporation rate, as demonstrated by Baldelli et al. [55]. The main advantage of the chain of droplets technique is the small size of the droplets (compared to the other single droplet drying methods) and the creation of monodisperse droplets. For example, Baldelli et al. [55] produced particles as small as 30 μm from an acetone droplet containing cellulose acetate butyrate. Regarding the particle size distribution, Rogers et al. [56] produced 100 μm particles with size variation smaller than 10 μm. In that way, the droplets generated will experience the same drying history and produce the same solid structures [92,93]. A few grams of powder can then be produced and used for the evaluation of powder bulk properties, like water content and solubility [92].

From the single droplet drying methods, droplet average parameters like mass, temperature and concentration can be obtained. Image analysis may also give evaporation rate from the isotropic shrinkage, if any, and external visualization of crust formation and evolution. To understand the mechanisms of component distribution during drying, many studies relate the changes in the initial droplet properties to the final particle properties, as shown in Table 3. This approach was previously discussed on the Section dedicated to the spray of droplets. The studies with *in situ* droplet components distribution measurement are presented in the next Section.

#### 3.2.7. In situ component distribution evaluation

In order to assess the internal droplet composition profile without disturbing the drying process, it is important to use experimental techniques that interfere the least with the droplet compounds. The techniques in this Section rely mainly on the electromagnetic waves emitted from the compounds present in the droplet to give information about their distribution in the liquid.

The research group of Quiño et al. [94] has developed an experimental set-up that enables the acquisition of a one-dimensional concentration profile inside the droplet using Raman spectroscopy. A droplet containing a mixture of acetone and water was levitated through an acoustic levitator and a Nd:YVO4 laser operating at 532 nm was horizontally directed to the droplet. A CCD camera coupled with an spectrometer captured the Raman light scattered at an angle of 90° from the incident laser beam. Even though no solid particle was formed during the experiment, the set-up developed was still useful for seeing how the acetone concentration was distributed across the droplet (Fig. 4). The data were obtained every second and the concentration points were spaced at intervals of 120 μm. Enhancing the concentration profile near the droplet surface by increasing the number of measured concentration points is a complicated task due to light distortion near the liquid-air interface. The same group also used the Raman technique for measuring a concentration profile of a supercritical drying gel placed on a high-pressure chamber [95] and the composition of a pendant liquid droplet confined in a supercritical carbon dioxide environment [96].

When a laser beam is focused on the droplet, only a small percentage of the incident light is reflected as Raman light. As a result, very sensible detectors have to be used in order to quantify the weak signal as a compound concentration. Increasing the laser power to reduce measurement errors may induce liquid evaporation. This would deviate the drying experiment from the spray drying process.

Apart from the Raman technique, Lemoine and Castanet [97] also presented an optical technique, called the Rainbow refractometry, which is based on the droplet's refractive index. According to the authors, the dependence of the refractive index with the droplet's temperature and composition should be known. The main

**Table 3**
Some examples of single droplet studies relating the changes in drying conditions to the final particle properties.

| Authors | Method | Compounds | Objective | Outcome |
|---|---|---|---|---|
| Osman et al. [107] | Acoustic levitation | Colloidal suspension. Silica nanoparticles in water. | Investigation of the particle morphology by varying the size of the silica nanoparticles from 46 nm to 2.5 μm. | Drying the 46 nm silica resulted in a dense spherical particle, while the microsized silica originated a particle with a shape resembling the human red blood cells. |
| Fu et al. [65] | Thin filament | Suspension of silica nanoparticles and Eudragit RS 30D containing either Rhodamine B or sucrose as model drug. | Investigation of the final particle solid structure (porosity, component distribution, surface visual aspect) by changing the concentration of the model drug in the formulation (0, 5 μg $mL^{-1}$ or 1.5 mg $mL^{-1}$) | The particle solid structure with no model drug presented a porous region rich in Eudragit RS near the particle surface and a denser region rich in silica towards the core of the particle. The visual aspect of these two regions was not modified by the addition of the model drug. However, Rhodamine B was more concentrated at the porous region, while the sucrose was more homogeneously distributed. All the formulations resulted in a particle smooth surface, except the formulation with a high loading of Rhodamine B, which presented small wrinkles on the particle surface. |
| Shamaei et al. [22] | Thin filament | O/w emulsion. Walnut oil as dispersed phase. Skim milk solution as continuous phase. | Investigation of the effects of drying air temperature (80°C–140°C), total solid content (12%–30% w/w) and oil/wall material mass fraction (0.25–1 w/w) on the particle size and surface morphology. | The particle surface became less wrinkled with increasing temperature and oil/wall ratio. A reduction in surface roughness was obtained with higher total solid content. Bigger particles were obtained by increasing the studied parameters. |
| Sadek et al. [58] | Hydrophobic surface | Two aqueous solutions were prepared: one with whey protein isolate (WPI), and the other with native phosphocaseinates (NPC). | Analysis of the particle morphology and crust properties (buckling time and compression behavior) under the same drying conditions (air temperature at 20°C and relative humidity at 2%). | The WPI particle had a hollow morphology with a smooth surface while the NPC particle presented a wrinkled morphology. The surface of the NPC particle started to buckle after 11 min of drying and the crust tends to deform under stress. On the contrary, the WPI particle crust started to buckle after 30 min and it tends to fracture under stress. |
| Mondragon et al. [126] | Acoustic levitation | Colloidal suspension. Silica nanoparticles in water. | Inluence of the solid mass fraction (0.02 w/w - 0.2 w/w), drying temperature (80°C–120°C), droplet initial volume (0.3 μL–0.8 μL), pH value (2–10) and salt concentration (0mol $L^{-1}$–0.05mol $L^{-1}$) on the final particle size, shell thickness and mechanical strength. | The solid mass fraction and the initial droplet volume had a positive effect on the final particle size, on the particle shell thickness and on the mechanical strength. The pH value had a positive effect on the particle mechanical strength only at high solid mass fraction. The other tested parameters did not have any important influence on the particle size, shell thickness and mechanical strength. |
| Mondragon et al. [89] | Acoustic levitation | Porcelain tile suspensions (45% clays, 6% sand and 49% feldspars) in water. | Influence of varying initial solid mass fraction (0.65 w/w - 0.70 w/w), flocculation state (flocculated - deflocculated), porcelain tile size (1.95 μm–3.25 μm), air temperature (70°C–100°C) and initial droplet volume (0.4 μL–0.7 μL) on the particle porosity and mechanical strength. | The porcelain tile size and the initial solid mass fraction had a negative effect on the porosity but a positive effect on the particle mechanical strength. Increasing the air temperature also had a positive effect on the mechanical strength but not a relevant importance for the porosity. The deflocculated porcelain tiles improved the particle porosity and may improve the particle mechanical strength if a high initial solid mass fraction is used. |
| Rogers et al. [92] | Free-fall technique | Reconstituted skim milk and milk protein concentrated powders | Influence of varying the air inlet temperature (from 77°C to 180°C) on the solubility of the final particle. | The temperature had a negative impact on the solubility of the dried particles. Indeed, an increase in the air temperature produced insoluble material in the droplet liquid phase during drying. |

drawback of this technique is the need of a transparent droplet. For this reason, this method would not be useful for the main dried systems, like emulsions and solid suspensions, as the presence of undissolved solids in the droplet would alter the liquid refractive index. Therefore, obtaining a concentration profile from the refracted light in such dispersion would be a quite complex task. Additionally, the formation of a solid crust, if not transparent, could impede the light from entering the droplet.

In the same publication [97], the use of laser-induced fluorescence to characterize the internal flowfield was also reported. Manukyan et al. [80] and Saha et al. [90] visualized the internal flow in a droplet deposited on a hydrophobic surface and a droplet acoustically levitated, respectively, by adding tracer nanoparticles in the droplet (copolymer [80] or polystyrene [90] microspheres). The former was interested in analyzing the effect of the initial contact angle and the pinning effect on the internal flow and the latter studied the effect of droplet size and viscosity on the internal flow. Even though this method does not give a direct measure of the component concentrations, it is a helpful technique to evaluate, for example, if the liquid streams could evenly homogenize the component concentrations, provided that the tracer employed does not disturb the drying process. According to Manukyan et al. [80], the weakening of the liquid streams after the crust formation could also be visualized.

Griffith et al. [98] employed nuclear magnetic resonance spectroscopy to study the drying of a detergent droplet suspended by a glass filament. A 10 μL-droplet (diameter around 1.6 mm) was excited at discrete times and the obtained spin echo profiles were translated into a water distribution profile. Despite its great potential, the use of this technique is not widespread due to capital expenditure (Capex) costs.

To evaluate the components distribution and the chemical surface composition of a droplet over discrete drying times, Foerster et al. [71] stopped the drying process by flash-freezing the droplet with a vial containing liquid nitrogen. Two model milk emulsions were studied, with different fat contents. The chemical surface composition of the frozen droplet was measured by X-ray spectroscopy, while the component distribution was assessed by confocal laser scanning microscopy. For the latter, the protein molecules were labelled with a red fluorescent dye and the fat with a green one. Then both were excited by respective laser lights. Compared to the methods presented in this Section, flash-freezing the droplet is a rapid way to stop the drying process and to allow a subsequently *ex-situ* measurement of the droplet component distribution.

## 4. Modeling approach for a single droplet

The representation of the drying process through models is an important tool to improve the knowledge about spray-dried particle formation. However, due to the complexity of the process, the model results have to be supported by experimental observations

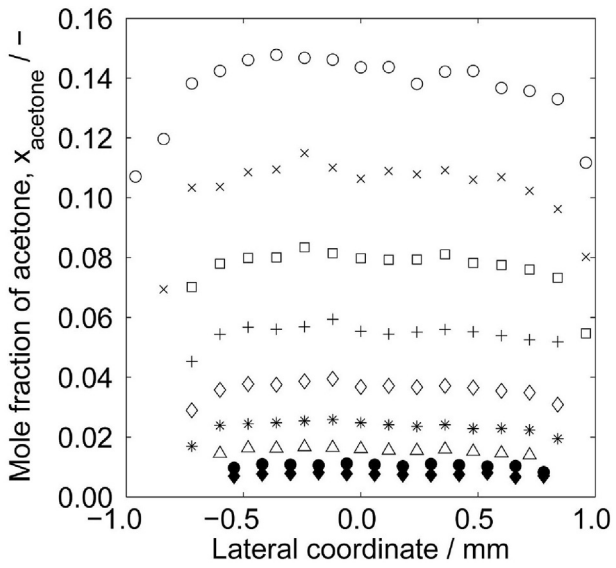


**Fig. 4.** Temporal evolution of radial composition profiles of a water-acetone droplet measured with the *in situ* Raman technique. From the lateral coordinate axis, the droplet initial diameter is about 2 mm and the final diameter is 1.3 mm. The acetone mole fraction difference between the droplet surface and center reduces over time. Adapted with permission from Ref. [94].

in order to be validated [62]. To adequately represent the drying of a multi-component droplet, a rigorous description of the component diffusive fluxes should be used, since the final component distribution strongly depends on how the substances are being transported in the liquid phase. The process of crust formation and development should be equally well described so that the models can properly represent the drying process of a droplet and then be scaled-up to represent the drying process at the industrial or commercial spray dryer scale.

The drying of a droplet has been illustrated through the use of an empirical or a deterministic approach. For the empirical approach (Section 4.1), experimental observations are used for describing the evolution of the droplet over time with average droplet properties (no spatial distribution). On the other hand, the deterministic approach (Section 4.2) uses spatially-resolved variables for representing the drying of the droplet, thus giving a much finer insight into the droplet variable changes.

### 4.1. Empirical approach

Three main empirical approaches have been used in the study of a single droplet drying: the characteristic drying curve (CDC) approach [99–101], the reaction engineering approach (REA) [100–106] and a Peclet number based analysis (PNA) [68,107].

The CDC and the REA approaches give fast information about the droplet drying kinetics. They are relatively simple to implement because they use lumped variables and the results can be quickly calculated. The parameters obtained with these two methods depend on the system dried and they do not give information about the particle morphologies [101]. More details about the CDC and REA models can be found in Ref. [100]. Mezhericher et al. [ [108] coupled the water vapor density at the surface of the droplet given by the REA approach to a continuous species transport approach (description in the next Section) to model the drying of a skim milk droplet. A good agreement was found between the model and the experimental results.

On the contrary, the PNA has been used to distinguish the final morphology of the dried particle. According to the value of the Peclet number, a dense core solid particle (Peclet inferior to 1) or a hollow particle (Peclet superior to 1) is expected. Indeed, the Peclet number takes into account the speed in which the droplet compounds diffuse in the droplet during drying and the speed at which the evaporation front recedes, that is to say a measure of the solid accumulation at the droplet surface [109]. Despite its relevance, this dimensionless parameter cannot be used to predict the formation of all the morphologies presented previously, since it does not give information about component distribution. Also, the Peclet number is calculated from the initial drying conditions, but its value may vary during the drying process because the diffusion coefficients and the evaporation front receding speed taken into account may change throughout the drying period. This approach was used by Chew et al. [110] on a series of experiments with a skim milk droplet suspended on the tip of a glass filament. From the plots of normalized particle diameter on the moisture content, the authors observed a deviation from the ideal shrinkage behavior (formation of dense particle) for high calculated Peclet numbers, indicating the formation of hollow particles.

### 4.2. Deterministic approach

Two main deterministic approaches have been used in the literature: the continuous species transport (CST) approach [60,108,111–118] and the CST approach coupled with a population balance [119–122].

The CST approach gives information about what happens inside the droplet during drying, since it uses spatially distributed variables. Even though this approach uses more complex equations and needs more time to give the results, the CST approach can be used to predict particle morphology [112]. The modeling of the first drying stage – where the activity coefficient of the solvent can be considered equal to one at the surface of the droplet – has been well supported by experimental data [60,108,112,115,120]. The droplet is considered to remain spherical, with no temperature gradient between its surface and the core and with an ideal shrinkage. The droplet properties are calculated only on the radial direction and the effect of the internal convection is often neglected [25,115,120]. Furthermore, the diffusion coefficient of the components in the droplet is expressed in terms of the Stokes-Einstein equation, which is a simpler equation valid for binary mixtures in infinite dilution. Such estimation may give a first idea of the value of the coefficient of diffusion for a higher water content, however as the concentration in the droplet increases, the values given by the Stokes-Einstein equation may be some orders of magnitude higher than a finer coefficient estimation [112,123].

Nevertheless, the description and experimental validation of the crust formation and growth are more challenging. The process of solid generation is generally overlooked by considering that the crust is formed once a certain saturation value [108,115] or a maximum packing fraction [25] are obtained. Handscomb et al. [121] considered a series of shell buckling and shrinkage events due to capillary forces on the droplet suspended solutes. This formation process takes place in only a few seconds, which makes experimental validation difficult.

The main morphologies represented in the literature with the CST approach are the dense and hollow morphologies with a rigid crust. The compounds present in the droplet are either solids in suspension or salts in solution. In that way, the crust formation comes from the agglomeration of the undissolved solids or through crystallization of dissolved crystal-forming compounds. To our knowledge, there is a lack when it comes to the description of the formation of an amorphous crust from substances completely dissolved in the liquid phase and the representation of wrinkled surfaces (apart from the description of the buckling process to form a doughnut-like particle).

Grasmeijer et al. [117] and Sadafi et al. [60,116] used the CST approach to model the drying of a dense particle. The glass transition temperature was used by Grasmeijer et al. [117] to determine the formation of a solid structure from a droplet containing a protein and a sugar. The droplet was subdivided in multiple subshells from the center of the droplet to its surface. Additionally, each subshell possessed homogeneous concentration. The obtained results were not experimentally validated. Due to recent advances in computer processing speed, this kind of model may be replaced by a more rigorous one. A different parameter is used by Sadafi et al. [60,116] to set the crust formation. They considered a critical concentration value for the crystallization of sodium chloride in water. The development of the crust on the surface of the droplet is calculated by blending the equations for the constant evaporation rate period and the falling rate period through a weighting factor. This factor varies from zero (no solid formed at the droplet surface) to one (surface covered by the solid surface). The modeling results were compared to experimental data obtained by the same team. The droplet evaporation rate was slightly underestimated compared to the experimental results.

The other particle morphology modeled by the CST approach is the hollow particle with rigid crust. It has been studied with the drying of a droplet containing silica nanoparticles in suspension [108,111–114]. Unlike the modeling of the dense particle, internal and external pressures across the wet particle are calculated during the formation of the solid crust for the hollow morphology. Indeed, at the surface of the droplet, liquid bridges between the nanoparticles create compressive tangential and radial stresses, leading to the formation of a crust when a maximum packing fraction value is reached. Once the crust is formed, the water vapor transfer through the pores of the crust is only dependent on the vapor concentration, because the pore size is considered to be much greater than the vapor molecular mean free path. Furthermore, Maurice et al. [114] state that the production of a hollow particle is possible when the solid crust generated at the surface of the droplet induces a reduction in the droplet internal pressure and thus the formation of a bubble, which may grow driven by the liquid evaporation. The model results concerning the bubble growth period was not validated by lack of experimental data.

Also on the formation of a hollow particle, Handscomb et al. [121] implemented a population balance in the CST approach to model the drying of a droplet containing a dissolved salt (with the hypothesis that one crystal seed is already present in the liquid phase) and nanoparticles in suspension and surrounded by stagnant air. The use of a population balance allowed the description of nanoparticle agglomeration, dissolved solid crystallization and the radial position of the suspended particles. The formation of the hollow particle could follow two routes from the developed model: a first one where the evaporation front recedes and water vapor diffuses through the pores of a dry crust, and a second one where the internal bubble growth keeps the evaporation front at the surface of the wet crust. Fickian diffusion was used for representing the movement of the compounds inside the droplet. Finally, a good agreement with experimental data was obtained from the modeling results.

## 5. Perspectives and conclusion

In the recent years, spray-drying has become a tool for producing particles with engineered end-use properties from multicomponent droplets. However, there is still a scientific challenge regarding the detailed description of the components distribution inside the droplet using either experimental approaches or models able of predicting the final particle solid structure from initial drying conditions and liquid formulation.

Experimental studies related to the spray of droplets only acquire information about the beginning and the end of the drying operation, with no follow-up of what occurs during the process. Single droplet methods have been developed to allow monitoring a simplified drying process, without any disturbances due to collisions. Those methods allow a measurement of the droplet average properties under well controlled drying conditions. They are capable of providing quantitative kinetic and morphological information necessary for the improvement of the drying models. Recently, experimental techniques using *in situ* electromagnetic waves were developed to obtain composition profiles inside the droplet. But so far, such profiles have not been obtained while the particle crust develops and grows. The use of such *in situ* techniques is indeed an interesting route to follow for obtaining critical information about the rearrangement of the components present in the droplet and further comprehension of the particle formation mechanisms.

Models have also been developed to demonstrate the evolution of the droplet properties and the apparition of two main solid morphologies: a dense and a hollow particle. The period of solid formation is generally overlooked in such models and the presence of compounds in the droplet is limited to solids in suspension or crystal-forming substances. The description of the process of amorphous solid formation from droplets containing multicomponents in solution is not well developed. Further improvement should equally be carried for emulsion droplets or multicomponent droplets containing porous nanoparticles in suspension. Compared to a solution droplet, modeling the finely dispersed liquid or solid phase inside the droplet would increase the complexity of the equations by the addition of multi-scale transport phenomena in the droplet. Another equally important parameter is the estimation of the diffusion coefficient. A fine description of the component's diffusion would be preferred, but such data, obtained theoretically or experimentally, would become complicated by increasing the number of constituents in the droplet.

## References


[1] J. Barbosa, P. Teixeira, Development of probiotic fruit juice powders by spray-drying: a review, Food Rev. Int. 9129 (2016) 1–24.
[2] M.-I. Ré, Formulating drug delivery systems by spray drying, Dry. Technol. 24 (2006) 433–446.
[3] M. Munoz-Ibanez, M. Nuzzo, C. Turchiuli, B. Bergenståhl, E. Dumoulin, A. Millqvist-Fureby, The microstructure and component distribution in spray-dried emulsion particles, Food Struct. 8 (2016) 16–24.
[4] R. Vehring, Pharmaceutical particle engineering via spray drying, Pharm. Res. 25 (2008) 999–1022.
[5] A. Paudel, Z.A. Worku, J. Meeus, S. Guns, G.V.D. Mooter, Manufacturing of solid dispersions of poorly water soluble drugs by spray drying : formulation and process considerations, Int. J. Pharm. 453 (2013) 253–284.
[6] R. Balgis, G.M. Anilkumar, S. Sago, T. Ogi, K. Okuyama, Rapid in Situ Synthesis of Spherical Microflower Pt/C Catalyst via Spray- Drying for High Performance Fuel Cell Application, 2012, pp. 665–669.
[7] F. Iskandar, Nanoparticle processing for optical applications – a review, Adv. Powder Technol. 20 (2009) 283–292.
[8] A. Stunda-Zujeva, Z. Irbe, L. Berzina-Cimdina, Controlling the morphology of ceramic and composite powders obtained via spray drying - a review, Ceram. Int. 43 (2017) 11543–11551.
[9] S.M. Thaker, P.A. Mahanwar, V.V. Patil, B.N. Thorat, P.A. Mahanwar, V.V. Patil, B.N.T. Synthesis, S.M. Thaker, P.A. Mahanwar, V.V. Patil, B.N. Thorat, Synthesis and Spray Drying of Water-Redispersible Polymer Synthesis and Spray Drying of Water-Redispersible Polymer, vol. 3937, 2010.
[10] M. Pal, L. Wan, Y. Zhu, Y. Liu, Y. Liu, W. Gao, Y. Li, G. Zheng, Scalable synthesis of mesoporous titania microspheres via spray-drying method, J. Colloid Interface Sci. 479 (2016) 150–159.
[11] S. Wanning, R. Süverkrüp, A. Lamprecht, Pharmaceutical spray freeze drying, Int. J. Pharm. 488 (2015) 136–153.
[12] W.D. Wu, K.C. Patel, S. Rogers, X.D. Chen, Monodisperse droplet generators as potential atomizers for spray drying technology, Dry. Technol. 25 (2007) 1907–1916.
[13] A. Sosnik, K.P. Seremeta, Advantages and challenges of the spray-drying technology for the production of pure drug particles and drug-loaded polymeric carriers, Adv. Colloid Interface Sci. 223 (2015) 40–54.
[14] S. Zellmer, G. Garnweitner, T. Breinlinger, T. Kraft, C. Schilde, Hierarchical structure formation of nanoparticulate spray-dried composite aggregates, ACS Nano 9 (2015) 10749–10757.

[15] H.M. Hassan, C.J. Mumford, Mechanisms drying of skin-forming materials. I.Droplets of material which gelatinised at high temperature, Dry. Technol. 11 (1993) 1713–1750.
[16] C. Sadek, P. Schuck, Y. Fallourd, N. Pradeau, C. Le Floch-Fouéré, R. Jeantet, Drying of a single droplet to investigate process–structure–function relationships: a review, Dairy Sci. Technol. 95 (2015) 771–794.
[17] J. Elversson, K. Andersson, A. Millqvist-Fureby, An atomic force microscopy approach for assessment of particle density applied to single spray-dried carbohydrate particles, J. Pharm. Sci. 96 (2007) 905–912.
[18] J. Elversson, A. Millqvist-Fureby, G. Alderborn, U. Elofsson, Droplet and particle size relationship and shell thickness of inhalable lactose particles during spray drying, J. Pharm. Sci. 92 (2003) 900–910.
[19] J. Elversson, A. Millqvist-Fureby, Particle size and density in spray drying - effects of carbohydrate properties, J. Pharm. Sci. 94 (2005) 2049–2060.
[20] H. Steckel, H.G. Brandes, A novel spray-drying technique to produce low density particles for pulmonary delivery, Int. J. Pharm. 278 (2004) 187–195.
[21] X. Li, N. Anton, T.M.C. Ta, M. Zhao, N. Messaddeq, T.F. Vandamme, Micro-encapsulation of nanoemulsions: novel Trojan particles for bioactive lipid molecule delivery, Int. J. Nanomed. 6 (2011) 1313–1325.
[22] S. Shamaei, A. Kharaghani, S.S. Seiiedlou, M. Aghbashlo, F. Sondej, E. Tsotsas, Drying behavior and locking point of single droplets containing functional oil, Adv. Powder Technol. 27 (2016) 1750–1760.
[23] A.B.D. Nandiyanto, K. Okuyama, Progress in developing spray-drying methods for the production of controlled morphology particles: from the nanometer to submicrometer size ranges, Adv. Powder Technol. 22 (2011) 1–19.
[24] J. Bahadur, D. Sen, S. Mazumder, B. Paul, H. Bhatt, S.G. Singh, Control of buckling in colloidal droplets during evaporation-induced assembly of nanoparticles, Langmuir 28 (2012) 1914–1923.
[25] M. Mezhericher, A. Levy, I. Borde, Modelling the morphological evolution of nanosuspension droplet in constant-rate drying stage, Chem. Eng. Sci. 66 (2011) 884–896.
[26] G. Marty, N. Tsapis, Monitoring the buckling threshold of drying colloidal droplets using water-ethanol mixtures, Europ. Phys. J. E 27 (2008) 213–219.
[27] L. Pauchard, Y. Couder, Invagination during the collapse of an inhomogeneous spheroidal shell, Europhys. Lett. 66 (2004) 667–673.
[28] C. Sadek, P. Schuck, Y. Fallourd, N. Pradeau, R. Jeantet, C. Le Floch-Fouéré, Buckling and collapse during drying of a single aqueous dispersion of casein micelle droplet, Food Hydrocolloids 52 (2016) 161–166.
[29] X. Chen, V. Boyko, J. Rieger, F. Reinhold, B. Reck, J. Perlich, R. Gehrke, Y. Men, Buckling-induced structural transition during the drying of a polymeric latex droplet on a solid surface, Soft Matter 8 (2012) 12093.
[30] D.H. Charlesworth, W.R. Marshall, Evaporation from drops containing dissolved solids, AIChE J. 6 (1960) 9–23.
[31] D.E. Walton, C.J. Mumford, The morphology of spray-dried particles: the effect of process variables upon the morphology of spray-dried particles, Chem. Eng. Res. Des. 77 (1999) 442–460.
[32] U.V. Shah, V. Karde, C. Ghoroi, J.Y.Y. Heng, Influence of particle properties on powder bulk behaviour and processability, Int. J. Pharm. 518 (2017) 138–154.
[33] P. Schuck, R. Jeantet, B. Bhandari, X.D. Chen, Í.T. Perrone, A.F. de Carvalho, M. Fenelon, P. Kelly, Recent advances in spray drying relevant to the dairy industry: a comprehensive critical review, Dry. Technol. 34 (2016) 1773–1790.
[34] D.L. Pearce, A novel way to measure the concentration of a spray in a spray dryer, Dry. Technol. 24 (2006) 777–781.
[35] W. Liu, X.D. Chen, C. Selomulya, On the spray drying of uniform functional microparticles, Particuology 22 (2015) 1–12.
[36] C. Sadek, H. Li, P. Schuck, Y. Fallourd, N. Pradeau, C. Le Floch-Fouéré, R. Jeantet, To what extent do whey and casein micelle proteins influence the morphology and properties of the resulting powder? Dry. Technol. 32 (2014) 1540–1551.
[37] E.M. Both, A.M. Karlina, R.M. Boom, M.A. Schutyser, Morphology development during sessile single droplet drying of mixed maltodextrin and whey protein solutions, Food Hydrocolloids 75 (2018) 202–210, https://doi.org/10.1016/j.foodhyd.2017.08.022.
[38] D. Heng, S.H. Lee, W.K. Ng, R.B.H. Tan, The nano spray dryer B-90, 2011, pp. 965–972.
[39] N. Fu, M.W. Woo, X.D. Chen, Single droplet drying technique to study drying kinetics measurement and particle functionality: a review, Dry. Technol. 30 (2012) 1771–1785.
[40] S. Nešić, J. Vodnik, Kinetics of droplet evaporation, Chem. Eng. Sci. 46 (1991) 527–537.
[41] T.M. El-Sayed, D.A. Wallack, C.J. King, Changes in particle morphology during drying of drops of carbohydrate solutions and food liquids. 1. Effect of composition and drying conditions, Ind. Eng. Chem. Res. 29 (1990) 2346–2354.
[42] S.X.Q. Lin, X.D. Chen, Improving the Glass-Filament Method for Accurate Measurement of Drying Kinetics of Liquid Droplets, vol. 80, 2002.
[43] J.-C. Lin, J.W. Gentry, Spray drying drop morphology: experimental study, Aerosol Sci. Technol. 37 (2003) 15–32.
[44] A.G. Marín, H. Gelderblom, A. Susarrey-Arce, A. van Houselt, L. Lefferts, J.G.E. Gardeniers, D. Lohse, J.H. Snoeijer, Building microscopic soccer balls with evaporating colloidal fakir drops, Proc. Natl. Acad. Sci. U.S.A. 109 (2012) 16455–16458.
[45] W. Xu, C.-H. Choi, Effects of surface topography and colloid particles on the evaporation kinetics of sessile droplets on superhydrophobic surfaces, J. Heat Transf. 134 (2012), 051022.
[46] P. Papadopoulos, X. Deng, L. Mammen, D.M. Drotlef, G. Battagliarin, C. Li, K. Müllen, K. Landfester, A. Del Campo, H.J. Butt, D. Vollmer, Wetting on the microscale: shape of a liquid drop on a microstructured surface at different length scales, Langmuir 28 (2012) 8392–8398.
[47] J. Perdana, M.B. Fox, M.A.I. Schutyser, R.M. Boom, Mimicking spray drying by drying of single droplets deposited on a flat surface, Food Bioprocess Technol. 6 (2013) 964–977.
[48] C. Groenewold, C. Möser, H. Groenewold, E. Tsotsas, Determination of single-particle drying kinetics in an acoustic levitator, Chem. Eng. J. 86 (2002) 217–222.
[49] A.L. Yarin, G. Brenn, O. Kastner, C. Tropea, Drying of acoustically levitated droplets of liquid-solid suspensions: evaporation and crust formation, Phys. Fluids 14 (2002) 2289–2298.
[50] R. Mondragon, L. Hernandez, J. Enrique Julia, J. Carlos Jarque, S. Chiva, B. Zaitone, C. Tropea, Study of the drying behavior of high load multiphase droplets in an acoustic levitator at high temperature conditions, Chem. Eng. Sci. 66 (2011) 2734–2744.
[51] M. Griesing, H. Grosshans, T. Hellwig, R. Sedelmayer, S. Gopireddy, W. Pauer, E. Gutheil, H.-U. Moritz, Influence of the Drying Air Humidity on the Particle Formation of Single Mannitol-Water Droplets, Chemie-Ingenieur-Technik submitted, 2015, pp. 1–9.
[52] B. Adhikari, T. Howes, B.R. Bhandari, V. Truong, Experimental studies and kinetics of single drop drying and their relevance in drying of sugar-rich foods: a review, Int. J. Food Prop. 3 (2000) 323–351.
[53] L. Hennet, V. Cristiglio, J. Kozaily, I. Pozdnyakova, H.E. Fischer, A. Bytchkov, J.W.E. Drewitt, M. Leydier, D. Thiaudière, S. Gruner, S. Brassamin, D. Zanghi, G.J. Cuello, M. Koza, S. Magazù, G.N. Greaves, D.L. Price, Aerodynamic levitation and laser heating: applications at synchritrin and neutron sources, Eur. Phys. J. Spec. Top. 196 (2011) 151–165.
[54] J.K.R. Weber, A. Tamalonis, C.J. Benmore, O.L.G. Alderman, S. Sendelbach, A. Hebden, M.A. Williamson, Aerodynamic levitator for in situ x-ray structure measurements on high temperature and molten nuclear fuel materials, Rev. Sci. Instrum. 87 (2016), 073902.
[55] A. Baldelli, M.A. Boraey, D.S. Nobes, R. Vehring, Analysis of the particle formation process of structured microparticles, Mol. Pharm. 12 (2015) 2562–2573.
[56] S. Rogers, W.D. Wu, S.X.Q. Lin, X.D. Chen, Particle shrinkage and morphology of milk powder made with a monodisperse spray dryer, Biochem. Eng. J. 62 (2012) 92–100, https://doi.org/10.1016/j.bej.2011.11.002. URL:.
[57] M. Foerster, T. Gengenbach, M.W. Woo, C. Selomulya, The impact of atomization on the surface composition of spray-dried milk droplets, Colloids Surfaces B Biointerfaces 140 (2016) 460–471.
[58] C. Sadek, L. Pauchard, P. Schuck, Y. Fallourd, N. Pradeau, C. Le Floch-Fouéré, R. Jeantet, Mechanical properties of milk protein skin layers after drying: understanding the mechanisms of particle formation from whey protein isolate and native phosphocaseinate, Food Hydrocolloids 48 (2015) 8–16.
[59] M. Eslamian, N. Ashgriz, Evaporation and evolution of suspended solution droplets at atmospheric and reduced pressures, Dry. Technol. 25 (2007) 999–1010.
[60] M.H. Sadafi, I. Jahn, A.B. Stilgoe, K. Hooman, A theoretical model with experimental verification for heat and mass transfer of saline water droplets, Int. J. Heat Mass Transf. 81 (2015) 1–9.
[61] M.A. Haque, B. Adhikari, A. Putranto, Predictions of drying kinetics of aqueous droplets containing WPI-lactose and WPI-trehalose by application of composite reaction engineering approach (REA), J. Food Eng. 189 (2016) 29–36.
[62] B. Adhikari, T. Howes, B.R. Bhandari, Use of solute fixed coordinate system and method of lines for prediction of drying kinetics and surface stickiness of single droplet during convective drying, Chem. Eng. Process: Process Intens. 46 (2007) 405–419.
[63] Y. Wang, L. Che, C. Selomulya, X.D. Chen, Droplet drying behaviour of docosahexaenoic acid (DHA)-containing emulsion, Chem. Eng. Sci. 106 (2014) 181–189.
[64] Y. Wang, L. Che, N. Fu, X.D. Chen, C. Selomulya, Surface formation phenomena of DHA-containing emulsion during convective droplet drying, J. Food Eng. 150 (2015) 50–61.
[65] N. Fu, W.D. Wu, M. Yu, F.T. Moo, M.W. Woo, C. Selomulya, X.D. Chen, In situ observation on particle formation process via single droplet drying apparatus: effects of precursor composition on particle morphology, Dry. Technol. 34 (2016) 1700–1708.
[66] I. Gouaou, M.S. Koutchoukali, A. Kharaghani, Experimental study of drying conditions on starch single droplet shrinkage and morphology during drying, in: Third International Conference on Energy, Materials, Applied Energetics and Pollution., 2016, pp. 326–332.
[67] S.X.Q. Lin, X.D. Chen, Changes in milk droplet diameter during drying under constant drying conditions investigated using the glass-filament method, Food Bioprod. Process. 82 (2004) 213–218.
[68] J.H. Chew, N. Fu, T. Gengenbach, X.D. Chen, C. Selomulya, The compositional effects of high solids model emulsions on drying behaviour and particle formation processes, J. Food Eng. 157 (2015) 33–40.
[69] N. Fu, M.W. Woo, C. Selomulya, X.D. Chen, Shrinkage behaviour of skim milk droplets during air drying, J. Food Eng. 116 (2013) 37–44.
[70] N. Fu, M.W. Woo, X.D. Chen, Colloidal transport phenomena of milk components during convective droplet drying, Colloids Surfaces B Biointerfaces

87 (2011) 255–266.
[71] M. Foerster, T. Gengenbach, M.W. Woo, C. Selomulya, The influence of the chemical surface composition on the drying process of milk droplets, Adv. Powder Technol. 27 (2016) 2324–2334.
[72] A. Al-Mubarak, M. Belkharchouche, M. Al-Hayan, A. Husain, Mechanisms of single droplet drying, Kuwait J. Sci. Eng. 37 (2010) 161–179.
[73] A. Saha, S. Basu, R. Kumar, Particle image velocimetry and infrared thermography in a levitated droplet with nanosilica suspensions, Exp. Fluid 52 (2012) 795–807.
[74] K. Han, G. Song, X. Ma, B. Yang, An experimental and theoretical study of the effect of suspended thermocouple on the single droplet evaporation, Appl. Therm. Eng. 101 (2016) 568–575.
[75] B. Ali Al Zaitone, C. Tropea, Evaporation of pure liquid droplets: comparison of droplet evaporation in an acoustic field versus glass-filament, Chem. Eng. Sci. 66 (2011) 3914–3921, https://doi.org/10.1016/j.ces.2011.05.011. URL:.
[76] C. Sadek, H. Tabuteau, P. Schuck, Y. Fallourd, N. Pradeau, C. Le Floch-Fouéré, R. Jeantet, Shape, shell, and vacuole formation during the drying of a single concentrated whey protein droplet, Langmuir 29 (2013) 15606–15613.
[77] J. Bouman, P. Venema, R.J. de Vries, E. van der Linden, M.A. Schutyser, Hole and vacuole formation during drying of sessile whey protein droplets, Food Res. Int. 84 (2016) 16.
[78] H. Al-Shehri, T.S. Horozov, V.N. Paunov, Preparation and attachment of liquid-infused porous supra-particles to liquid interfaces, Soft Matter 12 (2016) 8375–8387.
[79] M.A. Hampton, T.A.H. Nguyen, A.V. Nguyen, Z.P. Xu, L. Huang, V. Rudolph, Influence of surface orientation on the organization of nanoparticles in drying nanofluid droplets, J. Colloid Interface Sci. 377 (2012) 456–462.
[80] S. Manukyan, H.M. Sauer, I.V. Roisman, K.A. Baldwin, D.J. Fairhurst, H. Liang, J. Venzmer, C. Tropea, Imaging internal flows in a drying sessile polymer dispersion drop using Spectral Radar Optical Coherence Tomography (SR-OCT), J. Colloid Interface Sci. 395 (2013) 287–293.
[81] Z. Sun, L. Zhou, C. Xiao, X. Du, Y. Yang, Nanoparticle motion and deposition near the triple line in evaporating sessile water droplet on a super-hydrophilic substrate, Exp. Therm. Fluid Sci. 76 (2016) 67–74.
[82] A.G. Marín, H. Gelderblom, D. Lohse, J.H. Snoeijer, Order-to-disorder transition in ring-shaped colloidal stains, Phys. Rev. Lett. 107 (2011) 1–4.
[83] A. Khoufech, M. Benali, K. Saleh, Influence of liquid formulation and impact conditions on the wetting of hydrophobic surfaces by aqueous polymeric solutions, Chem. Eng. Res. Des. 110 (2016) 233–244.
[84] A. Khoufech, M. Benali, K. Saleh, Influence of liquid formulation and impact conditions on the coating of hydrophobic surfaces, Powder Technol. 270 (2015) 599–611.
[85] M. Damak, S.R. Mahmoudi, M.N. Hyder, K.K. Varanasi, Enhancing droplet deposition through in-situ precipitation, Nat. Commun. 7 (2016) 12560.
[86] H. Grosshans, M. Griesing, M. Mönckedieck, T. Hellwig, B. Walther, S.R. Gopireddy, R. Sedelmayer, W. Pauer, H.U. Moritz, N.A. Urbanetz, E. Gutheil, Numerical and experimental study of the drying of bi-component droplets under various drying conditions, Int. J. Heat Mass Transf. 96 (2016) 97–109.
[87] V. Cristiglio, I. Grillo, M. Fomina, F. Wien, E. Shalaev, A. Novikov, S. Brassamin, M. Réfrégiers, J. Pérez, L. Hennet, Combination of acoustic levitation with small angle scattering techniques and synchrotron radiation circular dichroism. Application to the study of protein solutions, Biochim. Biophys. Acta Gen. Subj. 1861 (2017) 3693–3699.
[88] M. Kreimer, I. Aigner, S. Sacher, M. Krumme, T. Mannschott, P. van der Wel, A. Kaptein, H. Schroettner, G. Brenn, J. Khinast, Mechanical strength of microspheres produced by drying of acoustically levitated suspension droplets, Powder Technol. 325 (2018) 247–260.
[89] R. Mondragon, J.C. Jarque, J.E. Julia, L. Hernandez, A. Barba, Effect of slurry properties and operational conditions on the structure and properties of porcelain tile granules dried in an acoustic levitator, J. Eur. Ceram. Soc. 32 (2012) 59–70, https://doi.org/10.1016/j.jeurceramsoc.2011.07.025. URL:.
[90] A. Saha, S. Basu, R. Kumar, Velocity and rotation measurements in acoustically levitated droplets, Phys. Lett. Sec. A: Gen. Atom. Solid State Phys. 376 (2012) 3185–3191.
[91] B. Pathak, S. Basu, Modulation of buckling dynamics in nanoparticle laden droplets using external heating, Langmuir 32 (2016) 2591–2600, https://doi.org/10.1021/acs.langmuir.6b00544.
[92] S. Rogers, Y. Fang, S.X. Qi Lin, C. Selomulya, X. Dong Chen, A monodisperse spray dryer for milk powder: modelling the formation of insoluble material, Chem. Eng. Sci. 71 (2012) 75–84, https://doi.org/10.1016/j.ces.2011.11.041. URL:.
[93] W.D. Wu, W. Liu, T. Gengenbach, M.W. Woo, C. Selomulya, X.D. Chen, M. Weeks, Towards spray drying of high solids dairy liquid: effects of feed solid content on particle structure and functionality, J. Food Eng. 123 (2014) 130–135.
[94] J. Quiño, T. Hellwig, M. Griesing, W. Pauer, H.U. Moritz, S. Will, A. Braeuer, One-dimensional Raman spectroscopy and shadowgraphy for the analysis of the evaporation behavior of acetone/water drops, Int. J. Heat Mass Transf. 89 (2015) 406–413.
[95] J. Quiño, M. Ruehl, T. Klima, F. Ruiz, S. Will, A. Braeuer, Supercritical drying of aerogel: in situ analysis of concentration profiles inside the gel and derivation of the effective binary diffusion coefficient using Raman spectroscopy, J. Supercrit. Fluids 108 (2016) 1–12.
[96] A. Braeuer, O.S. Knauer, J. Quiño, A. Leipertz, Quantification of the mass transport in a two phase binary system at elevated pressures applying Raman spectroscopy: pendant liquid solvent drop in a supercritical carbon dioxide environment, Int. J. Heat Mass Transf. 62 (2013) 729–740.
[97] F. Lemoine, G. Castanet, Temperature and chemical composition of droplets by optical measurement techniques: a state-of-the-art review, Exp. Fluid 54 (2013).
[98] J.D. Griffith, A.E. Bayly, M.L. Johns, Magnetic resonance studies of detergent drop drying, Chem. Eng. Sci. 63 (2008) 3449–3456.
[99] T.A.G. Langrish, T.K. Kockel, The assessment of a characteristic drying curve for milk powder for use in computational fluid dynamics modelling, vol. 84, 2001, pp. 69–74.
[100] K.C. Patel, X.D. Chen, Prediction of spray-dryied product quality using two simple drying kinetics models, vol. 28, 2005, pp. 567–594.
[101] X.D. Chen, S.X.Q. Lin, Air drying of milk droplet under constant and time-dependent conditions, AIChE J. 51 (2005) 1790–1799.
[102] X. Chen, G. Xie, Fingerprints of the drying behaviour of particulate or thin layer food materials established using a reaction engineering model, Food Bioprod. Process. 75 (1997) 213–222.
[103] Y. Jin, X.X.D. Chen, Numerical study of the drying process of different sized particles in an industrial-scale spray dryer, Dry. Technol. 27 (2009) 371–381.
[104] X. Yang, J. Xiao, M.-W. Woo, X.D. Chen, Three-dimensional numerical investigation of a mono-disperse droplet spray dryer: validation aspects and multi-physics exploration, Dry. Technol. 33 (2014), 141217112010003.
[105] O.A. George, X.D. Chen, J. Xiao, M. Woo, L. Che, Modeling and simulation of the polymeric nanocapsule formation process, AIChE J. 61 (2015) 4140–4151.
[106] K.C. Patel, X.D. Chen, S.X.Q. Lin, A composite reaction engineering approach to drying of aqueous droplets containing sucrose, maltodextrin (DE6) and their mixtures, AIChE J. 55 (2009) 217–231.
[107] A. Osman, L. Goehring, A. Patti, H. Stitt, N. Shokri, Fundamental Investigation of the Drying of Solid Suspensions, 2017.
[108] M. Mezhericher, A. Levy, I. Borde, Theoretical drying model of single droplets containing insoluble or dissolved solids, Dry. Technol. 25 (2007) 1025–1032.
[109] R. Vehring, W.R. Foss, D. Lechuga-Ballesteros, Particle formation in spray drying, J. Aerosol Sci. 38 (2007) 728–746, https://doi.org/10.1016/j.jaerosci.2007.04.005.
[110] J.H. Chew, M.W. Woo, X.D. Chen, C. Selomulya, J.H. Chew, M.W. Woo, X.D. Chen, C. Selomulya, Mapping the shrinkage behavior of skim milk droplets during convective drying mapping the shrinkage behavior of skim milk droplets during convective drying, Dry. Technol. 33 (2015) 1101–1113.
[111] M. Mezhericher, M. Naumann, M. Peglow, A. Levy, E. Tsotsas, I. Borde, Continuous species transport and population balance models for first drying stage of nanosuspension droplets, Chem. Eng. J. 210 (2012) 120–135, https://doi.org/10.1016/j.cej.2012.08.038. URL:.
[112] U. Maurice, M. Mezhericher, A. Levy, I. Borde, Drying of droplet containing insoluble nanoscale particles: numerical simulations and parametric study, Dry. Technol. 31 (2013) 1790–1807.
[113] U. Maurice, M. Mezhericher, A. Levy, I. Borde, Drying of droplets containing insoluble nanoscale particles: second drying stage, Dry. Technol. 33 (2015) 1837–1848.
[114] U. Maurice, M. Mezhericher, A. Levy, I. Borde, Particle Formation from Droplet Containing Nanoparticles : Internal Bubble Growth 3937, 2017.
[115] S. Shamaei, S.S. Seiiedlou, M. Aghbashlo, H. Valizadeh, Mathematical modeling of drying behavior of single emulsion droplets containing functional oil, Food Bioprod. Process. 101 (2017) 100–109.
[116] M.H. Sadafi, I. Jahn, A.B. Stilgoe, K. Hooman, Theoretical and experimental studies on a solid containing water droplet, Int. J. Heat Mass Transf. 78 (2014) 25–33.
[117] N. Grasmeijer, H.W. Frijlink, W.L.J. Hinrichs, Model to predict inhomogeneous protein-sugar distribution in powders prepared by spray drying, J. Aerosol Sci. 101 (2016) 22–33.
[118] J. Xiao, X.D. Chen, Multiscale modeling for surface composition of spray-dried two-component powders, AIChE J. 60 (2014) 2416–2427.
[119] P. Seydel, J. Blömer, J. Bertling, Modeling particle formation at spray drying using population balances, Dry. Technol. 24 (2006) 137–146.
[120] C.S. Handscomb, M. Kraft, A.E. Bayly, A new model for the drying of droplets containing suspended solids, Chem. Eng. Sci. 64 (2009a) 628–637.
[121] C.S. Handscomb, M. Kraft, A.E. Bayly, A new model for the drying of droplets containing suspended solids after shell formation, Chem. Eng. Sci. 64 (2009b) 628–637.
[122] C.S. Handscomb, M. Kraft, Simulating the structural evolution of droplets following shell formation, Chem. Eng. Sci. 65 (2010) 713–725.
[123] L. Malafonte, L. Ahrné, E. Kaunisto, F. Innings, A. Rasmuson, Estimation of the effective diffusion coefficient of water in skim milk during single-drop drying, J. Food Eng. 147 (2015) 111–119.
[124] S. Poozesh, N. Stiawan, F. Arce, P. Sundararajan, J.D. Rocca, A. Rumondor, D. Wei, R. Wenslow, H. Xi, S. Zhang, J. Stellabott, Y. Su, J. Moser, P.J. Marsac, Understanding the process-product-performance interplay of spray dried drug-polymer systems through complete structural and chemical characterization of single spray dried particles, Powder Technol. (2017) 685–695.
[125] D.A. LeClair, E.D. Cranston, Z. Xing, M.R. Thompson, Optimization of spray drying conditions for yield, particle size and biological activity of thermally stable viral vectors, Pharm. Res. 33 (2016) 2763–2776.
[126] R. Mondragon, J.E. Julia, A. Barba, J.C. Jarque, Microstructure and mechanical properties of grains of silica nanofluids dried in an acoustic levitator, J. Eur. Ceram. Soc. 32 (2012) 4295–4304.